MOLECULAR AND CELLULAR BIOLOGY, Sept. 2007, p. 6093–6102 Vol. 27, No. 17
0270-7306/07/$08.00+0 doi:10.1128/MCB.00789-07

Nap1l2 Promotes Histone Acetylation Activity during Neuronal Differentiation▽

Mikaël Attia,[1] Christophe Rachez,[2] Antoine De Pauw,[1]† Philip Avner,[1] and Ute Christine Rogner[1]*

Unité de Génétique Moléculaire Murine[1] and Unité Postulante de Régulation Epigénétique,[2] CNRS URA 2578, Institut Pasteur, 25 rue du Docteur Roux, 75724 Paris Cedex 15, France

Received 4 May 2007/Returned for modification 11 June 2007/Accepted 13 June 2007

The deletion of the neuronal *Nap1l2* (*n*ucleosome *a*ssembly *p*rotein *1-l*ike *2*) gene in mice causes neural tube defects. We demonstrate here that this phenotype correlates with deficiencies in differentiation and increased maintenance of the neural stem cell stage. Nap1l2 associates with chromatin and interacts with histones H3 and H4. Loss of Nap1l2 results in decreased histone acetylation activity, leading to transcriptional changes in differentiating neurons, which include the marked downregulation of the *Cdkn1c* (*c*yclin-*d*ependent *k*inase inhibitor *1c*) gene. *Cdkn1c* expression normally increases during neuronal differentiation, and this correlates with the specific recruitment of the Nap1l2 protein and an increase in acetylated histone H3K9/14 at the site of *Cdkn1c* transcription. These results lead us to suggest that the Nap1l2 protein plays an important role in regulating transcription in developing neurons via the control of histone acetylation. Our data support the idea that neuronal nucleosome assembly proteins mediate cell-type-specific mechanisms of establishment/modification of a chromatin-permissive state that can affect neurogenesis and neuronal survival.

Mammals possess three neuron-specific nucleosome assembly protein (NAP)-encoding genes, *NAP1L2* (29), *NAP1L3* (39), and *NAP1L5* (37), all of which are both intronless and monoallelically expressed. While the role of the ubiquitously expressed NAPs, NAP1 (NAP1L1) (15, 17, 19, 25, 35) and NAP2 (NAP1L4) (14, 26), in the assembly of nucleosomes and transport of histones has been extensively characterized, little is known about the role and functioning of neuron-specific NAP1-like proteins.

We previously showed that targeted deletion of the murine neuron-specific *Nap1l2* (*n*ucleosome *a*ssembly *p*rotein *1-l*ike *2*) gene leads to embryonic lethality from mid-gestation phase onwards, with surviving mutant chimeric embryos showing extensive surface ectoderm defects and open neural tubes similar to those observed in humans with spina bifida and anencephaly. These developmental defects were attributed to the overproliferation of neural precursor cells that is thought to be associated with the absence of *Nap1l2* activity (27). The present study aimed to understand the cellular and molecular mechanisms underlying this knockout phenotype.

Here we show by ex vivo differentiation studies of embryonic stem (ES) cells from which *Nap1l2* was deleted that *Nap1l2* regulates the kinetics of neuronal differentiation. In the absence of *Nap1l2*, neural precursors exhibit a diminished capacity for differentiation, an increase in proliferation, and increased levels of apoptosis. These effects of *Nap1l2* deletion are associated with a global decrease in cellular levels of histone acetyltransferase (HAT) activity. This finding is supported by observations that the highly acidic Nap1l2 protein colocalizes to the chromatin in the neuronal nucleus, binds to histones H3 and H4 in vitro, and increases HAT activity. Loss of Nap1l2 results in extensive changes in the transcriptional profile of neural precursor cells, with genes such as *Cdkn1c*, involved in neuronal differentiation, being affected. Not only can Nap1l2 be recovered in association with the transcription start site of *Cdkn1c* but also the deletion of Nap1l2 reduces histone H3 acetylation at the *Cdkn1c* promoter. Our data suggest strongly that Nap1l2 is implicated in the epigenetic regulation of gene expression occurring during neuronal differentiation and provide novel insights into the functions of tissue-specific members of the NAP family.

MATERIALS AND METHODS

Knockout construction. The 46C ES cell line was kindly provided by Austin Smith (43). A 10-kb genomic DNA fragment containing the entire *Nap1l2* gene was cloned into pBluescript SK(+) (Stratagene) by using the restriction enzymes NotI and XhoI (27). A herpes simplex virus thymidine kinase cassette was inserted into the XhoI site, and a *loxP* site was inserted into the PmlI site 5′ of the *Nap1l2* promoter. A hygromycin resistance gene flanked by two *loxP* sites was inserted into the PacI site 3′ of the *Nap1l2* gene, which is located 5′ and outside of the last exon of the *Ppnx* gene (9). The construct was then inserted into the 46C ES cell line by homologous recombination. The hygromycin resistance cassette, alone or together with the *Nap1l2* gene, was removed by transient transfection with the pCre-Pac plasmid (38). The correct integration of the construct and *loxP* sites and absence of the Cre-expressing plasmid in ES cell clones were verified by PCR and Southern blotting. Unless otherwise stated, three independent 46CΔ*Nap1l2* clones, termed C8, B2, and E2, were compared to the 46C*loxPNap1l2loxP* clone E1 for phenotypic analysis. The clones with *Nap1l2* deleted and the *Nap1l2*-floxed clones were used at similar cell passage numbers and were differentiated in parallel.

ES cell culture and differentiation into neurons. N2B27 medium was prepared as originally described (43). Differentiation was initiated in bacterial dishes, with 5×10^6 cells per B10 petri dish. Starting with embryoid body formation in suspension culture, 8 to 12 days of culture were required to enrich the cultures in 60% to 70% of neural stem cells. These cultures could be further enriched (up to 90%) by selection with 1 μg puromycin/ml for at least 4 days. Embryoid bodies were dissociated at the point of maximal expression of *Sox1*-green fluorescent protein (GFP) using Accumax (PAA Laboratories) and 5×10^6 neural precursor cells attached to poly-D-lysine (13.3 μg/ml phosphate-buffered saline [PBS] for 1 h)-pretreated 25-cm^2 cell culture dishes. When required, 20 μg/ml AraC

* Corresponding author. Mailing address: Unité Génétique Moléculaire Murine, CNRS URA 2578, Institut Pasteur, 25 rue du Docteur Roux, 75724 Paris Cedex 15, France. Phone: 33145688602. Fax: 33145688656. E-mail: urogner@pasteur.fr.

† Present address: Génétique Oncologique, Institut Curie, 26, rue d'Ulm, 75248 Paris Cedex 5, France.

▽ Published ahead of print on 25 June 2007.

(Sigma) was added for 48 h 5 days after attachment of the cells to eliminate proliferative cells from the cultures. The differentiated cells were almost exclusively neuronal with only a few astrocytes (glial fibrillary acidic protein [GFAP]-positive) detectable 5 days after attachment of the cultures. Neurons could be maintained for at least 2 weeks after attachment. In some experiments, untreated embryoid bodies were maintained in suspension culture for about 3 weeks. When appropriate, neural stem cells were treated with 100 ng/ml trichostatin A (TSA) for 24 h. The increase in HAT activity was monitored by Western blot analysis using an anti-acetyl histone H3 antibody.

Immunofluorescence. Subconfluent cells (70 to 80%) were grown directly on 9-cm^2 slide flasks (Nunclon). Cells were fixed using 2% paraformaldehyde in PBS for 20 min at room temperature (RT), then treated with 0.1% Triton X-100 in PBS for 2 min, and rinsed once with PBS. First and secondary antibodies were diluted 1:200 to 1:400 in PBS and incubated for 1 h at RT. Three 5-min washes with PBS were carried out after each incubation step. The cells were embedded in Vectashield with DAPI (4′,6′-diamidino-2-phenylindole; Vector) and visualized using a fluorescence microscope (Zeiss) equipped with SmartCapture software (Vysis).

Fluorescence-activated cell sorter (FACS) analyses were performed using a FACScan (BD Bioscience). Percentages of GFP-positive cells were determined after acquisition of 10,000 live cells using the Cell Quest 3.3 software (BD Bioscience). Cell tracer labeling was done using CellTrace Far Red DDAO-SE (Molecular Probes) at 25 μM in PBS–1% bovine serum albumin (BSA) for 10 min at 37°C. The reaction was stopped by the adding a threefold excess of ice-cold medium containing 20% fetal calf serum, and the cells were washed with PBS before FACS acquisition. The analysis was carried out on 10,000 *Sox1*-GFP-positive cells. DNA content analysis was carried out on 2×10^6 puromycin-selected neural precursor cells. Single-cell suspensions were incubated overnight at 4°C in 1 ml of 0.1% trisodium citrate dihydrate containing 0.1% Triton X-100, 100 μg/ml RNase, and 25 μg/ml propidium iodide (Sigma). FACS acquisition and analysis were performed on 30,000 live cells. Apoptosis assays were carried out using the annexin V-PE apoptosis detection kit I (BD Bioscience) according to the manufacturer's instructions. The FACS analysis was carried out on 10,000 cells.

RNA preparation and cDNA synthesis. Total RNA was prepared by using RNABle (Eurobio) and RNA quality examined using an Agilent 2100 bioanalyzer (Agilent). Random cDNA synthesis was carried out on 10 μg total RNA by using Moloney murine leukemia virus reverse transcriptase (Invitrogen) according to the manufacturer's conditions.

Quantitative PCR was performed using an ABIPRISM 7700 sequence detector and SYBR green PCR master mix (PE Biosystems) according to the manufacturer's conditions. Primers were designed using PrimerExpress software and used at optimal concentrations. Quantification of the amplification product was performed using the comparative threshold cycle method and the *Arpo* (*a*cidic *r*ibosomal phosphoprotein *PO*) gene as the gene expression reporter. We found that *Arpo* expression was stable during neuronal ex vivo differentiation and independent of *Nap1l2* expression. Sequences of the oligonucleotides used were as follows: for *Nap1l2*, 5′CAGACCGTCCAAAAGGACTTA3′(forward) and 5′AGTAAGGGTTGGTACATTTCA3′(reverse); for *Oct4*, 5′CTCACCCTGGGCGTTCTCT3′(forward) and 5′GGCCGCAGCTTACACATGTT3′(reverse); for *Nestin*, 5′CTCCTGTGACAGCCTTTCTGAAG3′ (forward) and 5′AGGATAGGGAGCCTCAGACATAGG3′ (reverse); for the ß-*III-tubulin* gene, 5′CCCCATTTTAGCCACCTCTGT3′(forward) and 5′TACCCCTCCCCCCGAATAA3′(reverse); for *Cdkn1c*, 5′AGAACCGCTGGGACTTCAACT3′(forward) and 5′GTAGAAGGCGGGCACAGACT3′(reverse); and for *Arpo*, 5′TCCAGAGGCACCATTGAAATT3′(forward) and 5′TCGCTGGCTCCCACCTT3′(reverse).

Microarray analysis was carried out using Agilent 8k mouse cDNA and Agilent 22k mouse development oligonucleotide arrays. Ten micrograms of total ARN was directly transcribed and Cy3 or Cy5 labeled and hybridized as indicated by the manufacturer. Data from scans were analyzed using Feature Extraction (version 7) and Rosetta software and annotated using SOURCE software (provided by the Genetics Department of Stanford University).

Expression constructs. The *Nap1l2* coding sequences were PCR amplified from genomic DNA and cloned into the BamHI and BglII sites of pEGFP-C1 (Clontech) or into the XhoI and XbaI sites of pcDNA3.1/HISA (Invitrogen), or into BglII and XbaI sites of p3xFLAG-CMV24 (Sigma). The HA-p300 pCMV vector was obtained from Upstate.

Transient transfection of neurons with plasmid DNA was carried out using Lipofectamine Plus (Gibco) according to the manufacturer's instructions. Alternatively, neurons were transfected with a construct containing the entire FLAG-tagged *Nap1l2* gene (see "Knockout construction" above) by using the Nucleofection method (Program C20, Nucleofector kit V; Amaxa). HeLa cells were cultured in Dulbecco's modified Eagle's medium (Gibco) supplemented with 10% fetal calf serum (Sigma). Transfections of p3xFLAG expression vectors were carried out in six-well plates by using polyethyleneimine (Exgen500; Euromedex) according to the manufacturer's instructions.

Antibodies. Polyclonal antibodies were raised in rabbits against Nap1l2-specific peptide N-terminal sequence Ala-Glu-Ser-Val-Asp-His-Lys-Glu-Leu-Ser-Glu-Ser-Asn-Gln-Glu (NeoMPS SA, Strasbourg, France) and were purified against the peptide by use of the Aminolink kit from Pierce. Specificity of the anti-Nap1l2 antibodies was tested by Western blotting using whole tissue extracts from brains and from COS7 cells overexpressing the 52-kDa Nap1l2 protein. Specific competition assays for the 1:1,000 diluted antisera were performed using 10 μg/ml of the appropriate peptide and a 30-min preincubation on ice. The anti-Nestin antibody Rat401 was from DSHB, anti-β-III-tubulin and anti-microtubule-associated protein 2 (anti-MAP2) antibodies were from Sigma, anti-GFAP antibody was from DAKO, while the anti-histone H3 and anti-p300 antibodies were all from Upstate. Anti-HA.11 antibodies were from COVANCE, and anti-FLAG antibodies were from Sigma.

Western blotting. Cytosolic and chromatin-containing nuclear extracts were prepared as described previously (21). Cellular extracts were separated on denaturing 12% polyacrylamide gels and blotted on Hybond C pure (Amersham) membranes. After transfer, the blots were blocked with 5% skim milk in water or in PBS containing 0.05% Tween 20 (PBS-Tween 20) for 30 min at RT and rinsed three times with PBS-Tween 20. Primary antibodies were diluted according to the manufacturer's indications. Polyclonal antisera against Nap1l2 were diluted 1:1,000 in PBS-Tween 20. After a one-hour incubation and three washes in PBS-Tween 20, the secondary peroxidase-coupled antibody (Sigma) was applied at a 1:2,000 dilution for 1 h at RT. After three washes in PBS-Tween 20, the blots were revealed using the ECL+ kit (Amersham).

Far-Western analysis was performed using 3 μg of purified histones (Roche and Upstate) separated on denaturing 15% polyacrylamide gels. After transfer to Hybond C pure nitrocellulose (Amersham), membranes were regenerated in PBS, 5% BSA, 0.05% Tween 20, and 1% fetal calf serum. Nap1l2 or luciferase was translated in vitro by using the coupled TnT kit (Promega) in the presence of [^{35}S]methionine (Amersham) and pcDNA-Nap1l2 or a luciferase expression vector. The radiolabeled proteins were then incubated with the membrane for 2 h at RT in the same buffer. After the membranes were washed, the signals were analyzed using a phosphorimager and Storm scanner control software. Signals were quantified using ImageQuant software (Amersham).

HAT assays were performed for 30 min at 30°C in 30 μl of 100 mM Tris-HCl, pH 8, 5% glycerol, 0.1 mM EDTA, 50 mM KCl, 1 mM dithiothreitol, 10 mM sodium butyrate, and 1 mM phenylmethylsulfonyl fluoride (HAT buffer) containing 0.25 μCi of [^{3}H]acetyl coenzyme A (MP Biomedicals) and 10 μg of histones (Roche). Depending on the experiment, the reaction mix was supplemented with immunoprecipitated Nap1l2 and/or p300 (each with 300 ng protein as the input), 2 μg of recombinant p300 (HAT domain; Upstate) or 2 μg of cellular extract, corresponding to the supernatant of cells incubated for 1 h at 4°C in HAT buffer containing 150 mM KCl and 0.5% NP-40. Protein concentrations were determined by Bradford assay (Bio-Rad). Fifteen microliters of the reaction mix was applied to P81 paper (Whatman). Scintillation counting of the air-dried membranes was performed for 1 min after three washes in 50 mM Na_2CO_3-$NaHCO_3$ buffer at pH 9.2 and one wash in acetone.

Immunoprecipitation assays. Extracts of transfected HeLa cells were prepared in 0.25 ml of lysis buffer containing 10 mM Tris-HCl, pH 7.5, 150 mM NaCl, 3 mM $MgCl_2$, 0.5% NP-40, protease inhibitors (Roche), and 0.1 U DNase I (Sigma). After centrifugation, the cleared extracts were diluted five times in lysis buffer without NP-40 and incubated at 4°C for 3 h with 40 μl of a 50% suspension of anti-FLAG M2 affinity resin (Sigma) equilibrated in lysis buffer with 0.1% NP-40. After four washes with lysis buffer containing 0.15% NP-40, samples were resolved on a 10% sodium dodecyl sulfate-polyacrylamide gel and detected by Western blotting.

Chromatin immunoprecipitation (ChIP) assays were done as previously described (22). Primers for quantitative PCR were as follows: for *Cdkn1c* position A, 5′AAGAACTCTGGGCTTCGGCT3′(forward) and 5′TCCGGTTCCTGCTACATGAAC3′(reverse); for *Cdkn1c* position B, 5′GGCAGATACTTAGGCCTGGGT3′(forward) and 5′GGCAGTACCGTGGCTGGAT3′(reverse); for *Cdkn1c* position C, 5′CCCTCCTCCTCTCCCCTCT3′(forward) and 5′CAGCGAGAAAGAAGGGAACG3′(reverse); for *Cdkn1c* position D, 5′TCCTCCCGTTCCCTTCTTTC3′(forward) and 5′GGTCGAAGGCTGTGCAAA3′(reverse); for *Cdkn1c* position E, 5′TCACCTTCTCGACTCCCTGC3′(forward) and 5′TACCGCCGCCAAAAGGA3′(reverse); for *Arpo*, 5′CCAATAGGCATGGACGACGT3′(UP2) and 5′CCCGCGTGTGCCTTTTATAG3′(LO2); for the ß-*actin* gene, 5′CCGTTCCGAAAGTTGCCTT3′(UP3) and 5′CGCCGCCGGGTTTTATA3′(LO3); and for *Nanog*, 5′GAGGATGCCCCCTAAGCTTTCCCTCCC3′(UP2) and 5′CCTCCTACCCTACCCACCCCCTATTCTCCC3′(LO2).

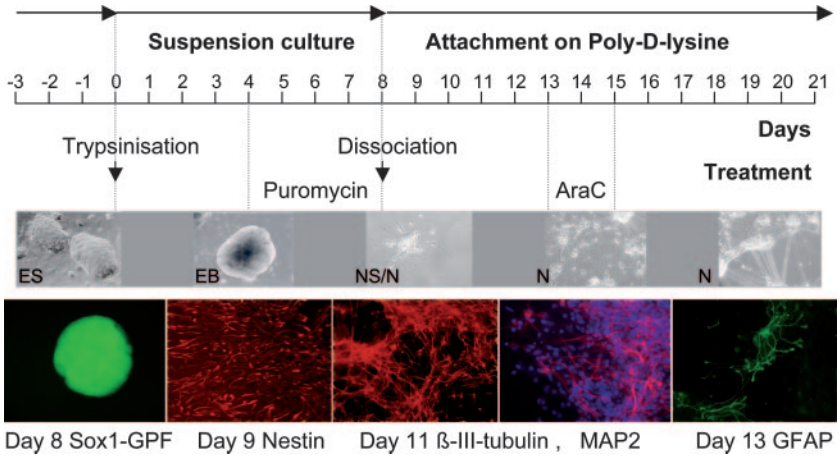

FIG. 1. Schematic description of the neuronal differentiation protocol. Different treatments and culture supports during a typical 21-day period of differentiation are shown. EB, embryoid body; NS, neural stem cell; N, neuron. The lower panels show examples of *Sox1*-GFP-expressing cells in embryoid bodies and immunofluorescence detection of the neural markers Nestin, β-III-tubulin (both in red), MAP2 (red), DAPI (blue), and GFAP (green).

Microarray data accession number. Raw experimental data from the microarray experiments have been submitted to the MIAMExpress database under accession number E-MEXP-1002.

RESULTS

***Nap1l2* knockout neural stem cells are delayed in neuronal differentiation.** Detailed study of the previously described *Nap1l2* deletion phenotype (27) required the establishment of an ex vivo cellular system allowing purified populations of neural stem cells and neurons to be isolated. To this end, we used the 46C ES cell line carrying the GFP gene and a puromycin resistance gene targeted to the *Sox1* locus (43). *Sox1* is one of the earliest neural markers, and the 46C ES cell line allows the identification and selection of GFP-positive neural stem cells during differentiation by FACS and/or puromycin selection (3). Enriched precursor cells can then be differentiated into neurons (Fig. 1).

The expression level of the pluripotent ES cell marker *Oct4* decreased rapidly during differentiation into neural precursor cells (Fig. 2). Conversely, the levels of the neural stem cell markers *Nestin* (Fig. 2) and *Sox2* (not shown), a transcription factor known to promote neural stem cell renewal (11), both increased during the period of suspension culture, when stem cells are accumulating. After attachment, the presence of *Sox1*-GFP- and *Nestin*-positive cells diminished within several days, while cells expressing the early neuronal marker β-III-tubulin could be detected by immunofluorescence within 24 h. Both β-III-tubulin- and MAP2-positive neurons were maintained in the attached cultures.

Both ES cell clones from which *Nap1l2* was deleted (46CΔ*Nap1l2*) and *Nap1l2*-floxed (46C*loxPNap1l2loxP*) ES cell clones were derived from the original 46C ES cell line by homologous recombination. Immunofluorescence studies using neural and neuron-specific markers showed that the *Nap1l2* deletion did not block the differentiation of ES cells into neural stem cells or neurons. To examine eventual quantitative effects of the deletion on the differentiation process, the *Oct4*, *Nestin*, *Sox2*, and β-*III-tubulin* gene markers were followed by real-time PCR. All three clones from which the *Nap1l2* gene was deleted expressed higher levels of *Nestin* (Fig. 2; see below) and *Sox2* (data not shown) notably during the suspension culture phase of differentiation. This apparent increase in neural precursor cells is in agreement with previous data that we have published on the in vivo and ex vivo effects of the *Nap1l2* knockout (27). Once attached, however, cells from all three clones from which *Nap1l2* was deleted expressed reduced levels of β-*III-tubulin* (the level for clone C8 was 45%, that for clone B2 was 53%, and that for clone E2 was 58% compared to the control level at day 11). This suggests that while the 46CΔ*Nap1l2* clones produce increased numbers of neural stem

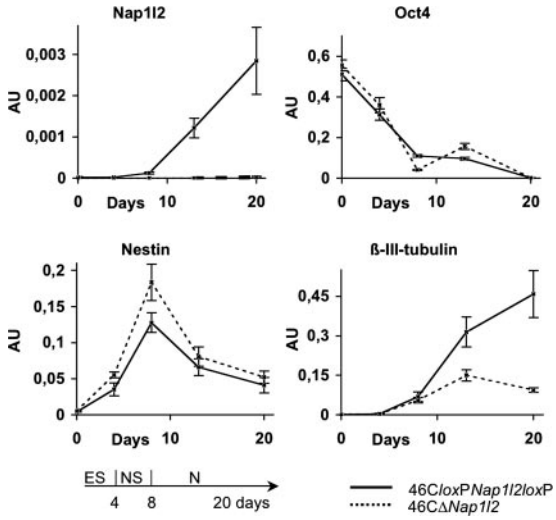

FIG. 2. Differentiation deficiencies of ES cells from which *Nap1l2* was deleted. Real-time PCR kinetics of *Nap1l2*, *Oct4*, *Nestin*, and β-*III-tubulin* expression during neuronal differentiation of wild-type cells (46C*loxPNap1l2loxP*; solid lines) and cells from which *Nap1l2* was deleted (46CΔ*Nap1l2*; dashed lines) are shown. NS, neural stem cell; N, neuron; AU, arbitrary units. Means ± standard deviations (error bars) are shown.

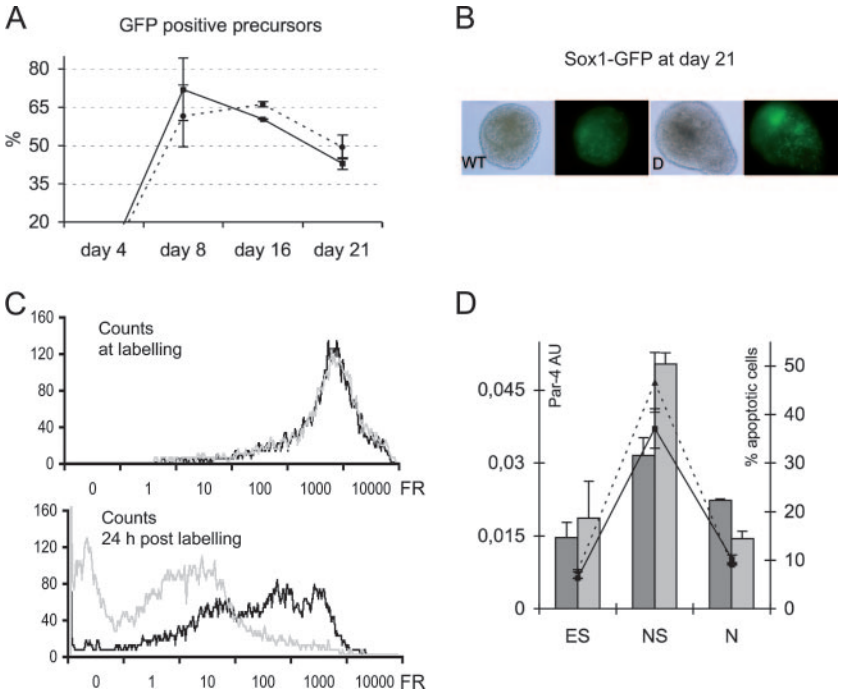

FIG. 3. Maintenance, proliferation, and apoptosis of neural precursors from which *Nap1l2* was deleted. (A) The percentages of *Sox1*-GFP-positive cells in suspension culture were analyzed by FACS. The data summarize three independent experiments using three different 46CΔ*Nap1l2* ES cell clones. Error bars represent standard errors of the means. (B) GFP expression in embryoid bodies of 46C*loxPNap1l2loxP* (WT) and 46CΔ*Nap1l2* cells (D) at day 21 is shown. (C) *Sox1*-GFP-positive cells were labeled using CellTrace Far Red DDAO-SE at day 10 of suspension culture, and the 24-h Far Red (FR) kinetics was analyzed by FACS. Results for wild-type cells are represented by dark lines, and results for mutant cells are represented by light-gray lines. Data are representative of two experiments. (D) Relative quantification in arbitrary units (AU) and standard deviations of *Par-4* expression by real-time PCR (bars) and determination of percentages of annexin V-positive cells by FACS (lines), given as the means ± standard errors of the means of two independent experiments, are shown for 46C*loxPNap1l2loxP* (dark bars and solid line) and 46CΔ*Nap1l2* cells (light bars and dashed line) at different stages of neuronal differentiation. NS, neural stem cell; N, neuron.

cells, their differentiation into neurons is less efficient. FACS analysis using an anti-β-III-tubulin antibody performed one day after cell attachment showed some 5% less β-III-tubulin-positive cells in cultures of the clones with deletions than the control culture, which contained some 40% β-III-tubulin-positive *Sox1*-GFP-negative cells. We conclude that *Nap1l2* deletion leads to less efficient differentiation of neural stem cells into neurons.

Proliferative changes in *Nap1l2* knockout neural precursor cells. We next turned our attention to estimating the survival of neural stem cells by analyzing the number of *Sox1*-GFP-expressing cells in suspension cultures. The control 46C*loxPNap1l2loxP* cell line and all three 46CΔ*Nap1l2* cell lines produced between 60% and 70% of neural precursor cells within 8 days of the initiation of differentiation. Typically in control cultures, the numbers of GFP-positive cells then decreased, dropping below 50% by day 21. However, in the 46CΔ*Nap1l2* cultures, the numbers of neural stem cells continued to increase until day 16 ($P < 0.03$ in unpaired Student's *t* test), and the clones with deletions showed a small but consistent increase (7%) in the number of precursor cells that was still detectable at day 21 (Fig. 3A and B). This suggests that deletion of the *Nap1l2* gene improves the capacity for neural stem cell renewal.

To test whether the cells from which *Nap1l2* was deleted had an enhanced capacity for cell division, we performed membrane-labeling experiments at day 10 of differentiation in suspension culture. The fluorescence intensity of the CellTrace dye, which is covalently bound to the cell membrane, diminishes by half at each cellular division. FACS analysis of nonsynchronized GFP-positive neural precursor cultures revealed that the 46CΔ*Nap1l2* cells lost fluorescence more rapidly during the initial 24 h of culture after labeling than control cells did, indicating that they had undergone more cellular divisions than the nonmutant cells or that they contained more dividing cells (Fig. 3C). We noted that, concomitant with these results, the level of *Ki67*, a marker of cycling cells, in the 46CΔ*Nap1l2* neural precursor cultures showed a twofold increase (data not shown), while the expression of *Cdkn1c*, which promotes cell cycle exit, was markedly decreased (see below).

We tested the hypothesis that the increase in neural stem cell numbers in the mutant cultures was associated with changes in their cell cycle by use of FACS based on a comparative DNA content analysis of *Sox1*-GFP-positive cells. While two independent experiments showed a slight expression level increase in G_1 (or G_0) phase (for mutant and wild-type cells, respectively, 59% versus 62% of 30,000 propidium iodide-stained viable neural precursor cells per experiment) and decreases in the S (for mutant and wild-type cells, respectively, 17% versus 16.5%) and G_2/M phases (for mutant and wild-type cells, respectively, 18.5% versus 16.5%), overall, the cell cycle was not significantly altered in the neural stem cells with

TABLE 1. Summary of microarray results for genes strongly deregulated in the *Nap1l2* knockout neural precursors[a]

GenBank accession no.	Gene product	Gene	Chromosome[b]	Fold change in expression
AA437922	Neuronatin	*Nnat*	2 (88.0 cM)	+3,200
AI509951	Calcium channel, voltage-dependent, T type, alpha 1G subunit	*Cacna1g*	11 (D band)	+3,867
AA014727	Pleckstrin homology-like domain, family A, member 2	*Phlda2*	7 (69.5 cM)	−3,000
AA671166	Cyclin-dependent kinase inhibitor 1c (p57)	*Cdkn1c*	7 (69.49 cM)	−4,733
AA874599	Host cell factor C1	*Hcfc1*	X (29.54 cM)	−3,667
AI322387	Mouse insulin-like growth factor II	*Igf2*	7 (69.09 cM)	−4,767

[a] Genes with an average change in expression level (*n*-fold) greater than 3 are listed.
[b] cM, centimorgans.

Nap1l2 deleted compared to control cells (paired Student's *t* test). This result suggests that the increase in neural stem cell presence associated with the *Nap1l2* deletion is most likely due to increased stem cell renewal linked to a prolongation of the neural stem cell stage and a reduction in the differentiation capacity of the 46CΔ*Nap1l2* neural stem cells.

We next addressed the question of why the increase in neural precursor cells seen for clones with the *Nap1l2* deletion did not lead to an increased number of neurons. One possibility was that this could be associated with a concomitant increase in apoptosis of some fraction of the neural precursor cell population, for example, due to increased removal of damaged or misspecified cells that failed to undergo differentiation (42). To evaluate this possibility, we first tested expression of the *Par-4* (*P*rostate *a*poptosis *r*esponse *4*) gene. Par-4 is an inhibitor of the antiapoptotic caspase and is known to regulate neural precursor cell death during division through a mechanism involving the asymmetric distribution of Par-4 to cells that will undergo apoptosis (5). As expected, *Par-4* showed maximal expression in neural precursor cells (Fig. 3D) with 46CΔ *Nap1l2* cells showing significantly higher expression of this marker, indicative of increased levels of apoptosis. To confirm this observation, we performed an apoptosis assay using 7-amino-actinomycin D and annexin V-phycoerythrin staining. The FACS analysis, carried out in two independent differentiation experiments, revealed a 7 to 12% increase in the number of annexin V-positive cells undergoing apoptosis in the *Sox1*-GFP-positive 46CΔ*Nap1l2* population (Fig. 3D). We conclude that *Nap1l2* deletion both increases renewal of cells with neural stem cell characteristics and hampers via apoptotic mechanisms the passage of neural stem cells to form differentiated neurons.

***Nap1l2* deletion leads to transcriptional changes in neural precursor cells.** To assess the effects of *Nap1l2* deletion on gene expression, we performed microarray experiments using three independent preparations of puromycin-selected neural precursor cells. In each set of experiments, the control cell line 46C*loxPNap1l2loxP* was compared against one of the 46CΔ *Nap1l2* cell lines. All three experiments included dye swaps to minimize possible technical bias. Primary data were analyzed and normalized using Feature Extraction software and Rosetta software set to a *P* value smaller than 0.1. We found that 97 genes were upregulated and 128 downregulated in the mutant cell lines in all three experiments. This corresponds to a deregulation of some 3% of the analyzed gene complement, with 2.3% showing *P* values of less than 0.05 by Student's *t* test. The extension of the analysis to a mouse development oligonucleotide array carrying 20,000 probes has confirmed these results, with 309 genes shown to be downregulated and 474 genes upregulated (3.6%). Average changes (*n*-fold) were modest (<5), and no chromosomal or domain clustering was apparent for the deregulated genes. While the upregulation of certain neuronal markers, such as *Nestin* (1.7-fold) and *Sox2* (1.5-fold in the mutant), was confirmed, annotation of deregulated genes revealed that they were associated with a wide range of cellular functions rather than being restricted to neuron-specific expression and function. We conclude that the absence of *Nap1l2* in neural stem cells does not lead to a specific deregulation of neural-specific genes.

Only six known genes showed expression levels that were altered threefold or greater (Table 1). We identified among these downregulated genes *Cdkn1c* (*p57kip2*), a gene required for cell cycle exit and for postmitotic differentiation of neurons. Rothschild et al. (28) have previously shown both ex vivo and in vivo that *Cdkn1c* is expressed in differentiating neurons. Mice lacking the *Cdkn1c* gene exhibit altered cell proliferation, apoptosis, and differentiation (44). In agreement with this, Joseph et al. (16) and Park et al. (24) demonstrated by transfection experiments that Cdkn1c promotes cell cycle exit and neuronal development. Detailed analysis of the *Cdkn1c* expression in our system has confirmed that its expression was concomitant with the onset of both neuronal differentiation and *Nap1l2* expression (see Fig. 5A and B), suggesting that the downregulation of *Cdkn1c* might be of particular interest with respect to the *Nap1l2* deletion phenotype. We therefore tested whether *Cdkn1c* could be a direct target of Nap1l2.

Nap1l2 binds to the *Cdkn1c* target gene and increases the acetylation status of chromatin bound histone H3. Nap1l2 is mainly expressed in postmitotic neurons. Both, immunofluorescence studies using an anti-Nap1l2 antibody (Fig. 4A and B) and transient transfection with GFP-Nap1l2-expressing constructs showed that the Nap1l2 protein is enriched in the nuclear compartment of β-III-tubulin-positive neurons (Fig. 4B, C, and D). This suggests that the function of the Nap1l2 protein in neurons might be related to a nuclear, chromatin-associated activity. We turned to ChIP to study whether Nap1l2 binds effectively to chromatin using as the putative target gene *Cdkn1c* (*p57kip2*). Our studies showed that Nap1l2 is specifically recruited to the transcription start site of *Cdkn1c* in differentiating neurons (Fig. 5C and D). This binding of the Nap1l2 protein in differentiating neurons is associated with increased levels of acetylated histone H3K9/14 around the transcription start site of *Cdkn1c* (Fig. 5C and E). Since this histone modification effect was not associated with general

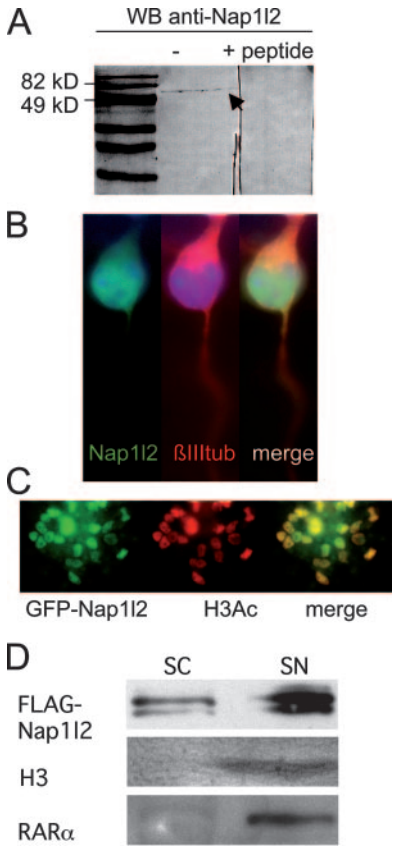

FIG. 4. Localization of Nap1l2 in neurons. (A) Western blot analysis using extracts from Nap1l2 (arrow)-expressing cells and the anti-Nap1l2 antibody (left) or the anti-Nap1l2 antibody preincubated with the Nap1l2 N-terminal peptide (right). (B) Immunofluorescence using an anti-Nap1l2 (green) and an anti-β-III-tubulin (βIIItub; red) antibody on differentiated neurons. DAPI staining is shown in blue. (C) Immunofluorescence of GFP-Nap1l2 (green)-transfected neurons with an anti-acetyl-H3K9/14 antibody (H3Ac; red). (D) Western blot analysis using fractions from FLAG-Nap1l2-transfected neurons and anti-FLAG, anti-histone H3, and anti-RARα antibodies. SC, soluble cytoplasmic extract; SN, soluble nuclear extract.

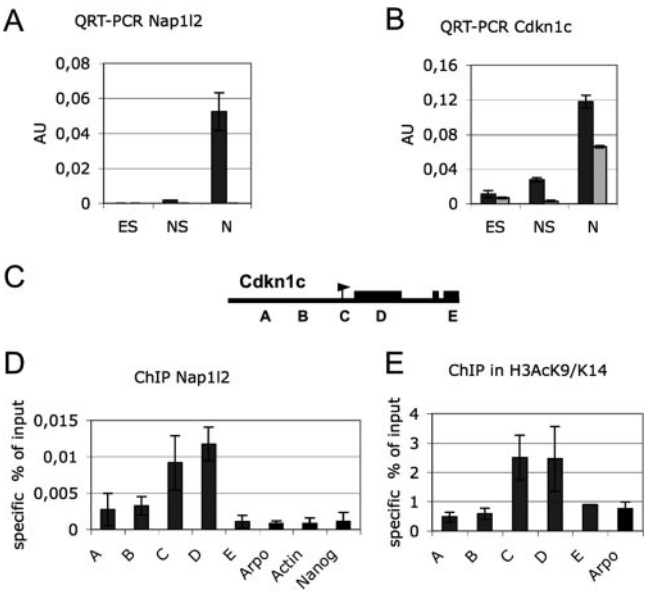

FIG. 5. *Cdkn1c* expression, Nap1l2 binding and histone H3 acetylation. Relative mRNA concentrations of *Nap1l2* (A) and *Cdkn1c* (B) were measured by quantitative real-time PCR (QRT-PCR). NS, neural stem cells; N, neurons. Values for controls are indicated by dark-gray bars, and values for mutant cells are indicated by light-gray bars. The experiment was repeated three times. (C) The relative positions of primer pairs A, B, C, D, and E in the *Cdkn1c* gene are shown with the transcription start indicated by an arrow and exons by black boxes. The lower panels show the specific binding of Nap1l2 to the *Cdkn1c* gene in wild-type neurons (summary of three independent experiment ± standard errors of the means [error bars]) (D), the gain in H3K9/14 acetylation on *Cdkn1c* in differentiated 46C*loxPNap1l2loxP* neurons compared to 46CΔ*Nap1l2* neurons (summary of two independent experiments ± standard errors of the means [error bars]) (E). The primers used for the control *Arpo*, β-*actin*, and *Nanog* genes are located at the transcription start.

changes in histone H3 levels (data not shown) and Nap1l2 itself is bound to *Cdkn1c*, it seems likely that these changes in H3 histone modifications were directly dependent on the presence of Nap1l2. We conclude that one mechanism by which Nap1l2 may regulate expression of target genes, such as *Cdkn1c*, is via regulation of histone acetylation.

The *Cdkn1c* gene is known to be subject to epigenetic regulation and can be activated by after TSA treatment (31). Histone acetylation has also been suggested as an epigenetic factor promoting neuronal differentiation (4, 13), and this correlates with an increase in the global pool of chromatin-bound acetylated histone H3 in differentiated neurons compared to neural stem cells and ES cells (Fig. 6A).

To test whether increased HAT activity could rescue *Cdkn1c* expression deficiency and the *Nap1l2* deletion phenotype during neuronal differentiation, we treated neural stem cells with the histone deacetylase inhibitor TSA for 24 h. Quantitative PCR results showed that *Cdkn1c* expression was strongly increased by TSA treatment in both the wild-type and mutant cells (Fig. 6B). Neural stem cells with *Nap1l2* deleted appeared to be more sensitive to TSA treatment than wild-type cells were. TSA also appeared to increase neuronal differentiation as shown by the expression of the marker β-*III-tubulin* gene (Fig. 6D). Interestingly, after TSA treatment, the β-*III-tubulin* levels of cells from which *Nap1l2* was deleted were even higher than those of nonmutant cells. This inverted kinetics may be interpreted as the consequence of the simultaneous differentiation of a larger number of neural stem cells in the mutant, which correlates with the observation that the previously described differences in *Nestin* expression (Fig. 2 and 6C) were abolished by TSA treatment (Fig. 6C). Our data suggest that the delay in differentiation associated with the *Nap1l2* deletion can be rescued by an increase in HAT activity. Our data are compatible with the idea that the *Nap1l2* deletion phenotype could be related to altered levels of HAT activity.

Nap1l2 binds to histones H3 and H4. We turned to ex vivo and in vitro studies to try to understand the basis for the Nap1l2-associated activities on HAT. By use of far-Western blotting and an in vitro-translated ^{35}S-radiolabeled Nap1l2 protein as a probe, Nap1l2 could be shown to interact with core histones, most strongly with histone H3 and to some extent also with histone H4 (Fig. 7A) but not with histones H2A and H2B or linker histones. We performed similar experiments

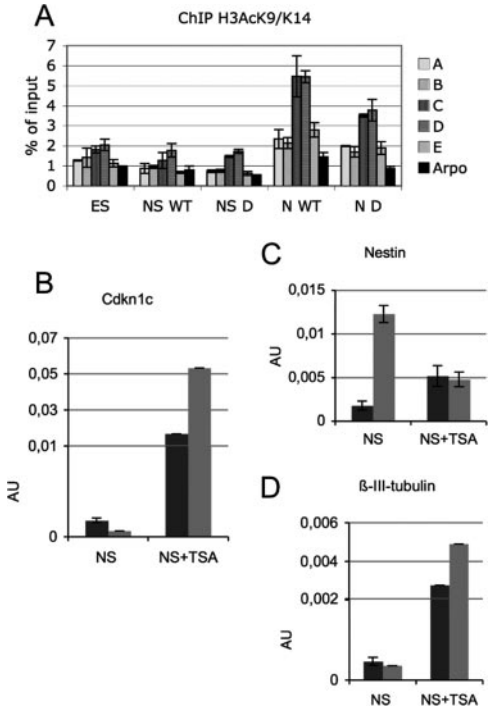

FIG. 6. Neuronal differentiation, histone acetylation, and *Cdkn1c* expression. (A) Kinetics of histone H3K9/14 acetylation on *Cdkn1c* (for primer positions, see Fig. 5) and *Arpo* during neuronal differentiation was determined by ChIP experiments. NS, neural stem cells; N, neurons. Means ± SD of two measurements are shown. Neural stem cells derived from 46C*loxPNap1l2loxP* (dark bars) and 46CΔ*Nap1l2* (light bars) cells were treated with 100 ng/ml TSA for 24 h. The relative mRNA levels for *Cdkn1c* (B), *Nestin* (C), and the β-*III-tubulin* genes (D) of all samples were determined 48 h after TSA treatment. The data are representative of two independent experiments. Results are given in arbitrary units (AU) ± SD.

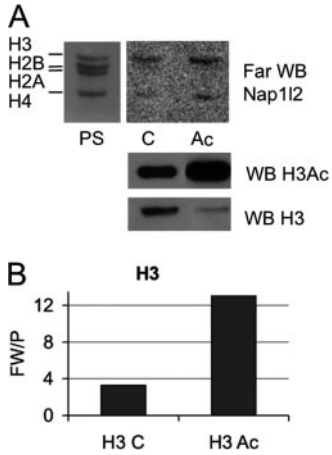

FIG. 7. Nap1l2 interaction with histones. (A) Far-Western blot analysis using a ^{35}S-radiolabeled Nap1l2 protein. Ponceau S staining (PS) and autoradiogram analysis reveal the interactions with histones H3 and H4 (C) and stronger interaction with acetylated histones H3 and H4 (Ac); results of one of three independent experiments are shown. Control Western blots (WB) for this experiment using anti-H3 and anti-acetyl-H3 antibodies are shown below. The calculated ratios of the far-Western signals for H3 against the Ponceau S signals (FW/P) are shown at the bottom of panel B.

using substrate pools enriched in acetylated histones, purified from butyrate-treated cells. In these experiments, Nap1l2 could be shown to bind preferentially to the acetylated forms of histones H3 and H4 (Fig. 7A and B).

Nap1l2 increases HAT activity. The increase in expression of *Nap1l2* parallels the increase in the global pool of chromatin-bound acetylated histone H3 in differentiating neurons (Fig. 6A). The preferential binding of Nap1l2 to histone H3 and its in vivo effect on the acetylation status of chromatin-bound histone H3 led us to examine whether Nap1l2 could be directly involved in the process of histone acetylation.

Using histone acetyltransferase assays of cellular extracts from differentiated neurons, at a stage when Nap1l2 is highly expressed, for a comparison of the Nap1l2-floxed control with *Nap1l2* knockout cells showed that extracts lacking Nap1l2 had lowered HAT activity (Fig. 8A). In another experiment in which either GFP or GFP plus Nap1l2 was overexpressed in neurons (Fig. 8B), overexpression of Nap1l2 again appeared to enhance the global HAT activity of the cellular extract. Similar observations were made using HeLa cells transfected with a Nap1l2-expressing construct (Fig. 8C). It is therefore likely that Nap1l2 participates in HAT complexes or facilitates access of such complexes to histones.

Other members of the NAP family, NAP1 (NAP1L1) and NAP2 (NAP1L4), are known to be functionally important components of the p300 coactivator complex suggesting that NAPs may serve as a point of integration between transcriptional coactivators and chromatin (2, 15, 34). Like other members of the NAP family, Nap1l2 contains a SET/TAF-1β oncoprotein domain, which has been shown to interact with p300 and to influence its HAT activity (33). Our preliminary results suggest that immunoprecipitated p300 from 46C*loxPNap1l2loxP* control neurons has a higher level of HAT activity than p300-containing complexes immunoprecipitated from neurons with *Nap1l2* deleted. This putative activation of p300 in the presence of Nap1l2 was confirmed by in vitro assays using immunoprecipitated Nap1l2 and both immunoprecipitated and recombinant p300 (data not shown). By use of coimmunoprecipitation assays using HeLa cells overexpressing Nap1l2 and p300, we were able to show that these proteins interact (data not shown). ChIP experiments using anti-p300 antibodies did not, however, provide any evidence that binding of p300 itself at the site of *Cdkn1c* transcription was dependent on Nap1l2 in neurons (data not shown). We conclude that Nap1l2 or Nap1l2-containing complexes stimulate HAT activity in neurons and have preliminary evidence that p300 may be part of these complexes.

DISCUSSION

We have shown that *Nap1l2* is implicated in the neural stem differentiation pathway and that deletion of *Nap1l2* leads to both delayed neuronal differentiation and increased neural precursor renewal, maintenance, and apoptosis. It appears likely that these cellular phenotypes are, at least in part, mediated by the effects of Nap1l2 downstream target genes showing altered transcriptional activity in cells with *Nap1l2* deleted. Among genes downregulated in neural precursors and neurons from which *Nap1l2* was deleted was the *Cdkn1c* gene, a nega-

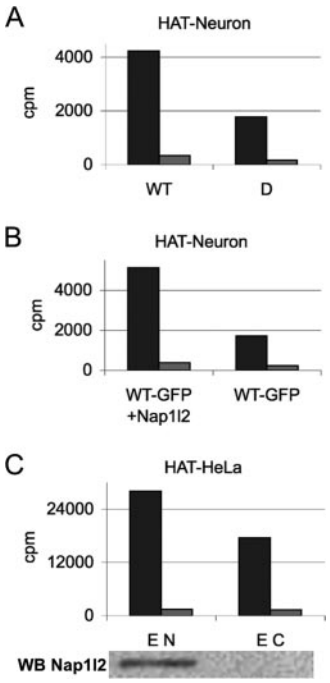

FIG. 8. HAT activity in the presence of Nap1l2. HAT assays using 2 μg of crude extract from control (WT) and Δ*Nap1l2* neurons (D) (panel A) or WT neurons overexpressing Nap1l2 and GFP or GFP alone (panel B). (C) HAT assays using HeLa cell extracts transfected with an empty 3× FLAG vector (E C) or with the 3× FLAG-Nap1l2 expression vector (E N). The result of the Western blot analysis (WB) using an anti-3× FLAG antibody is shown below. Dark-gray columns refer to cpm for the histone samples, and light-gray columns refer to cpm for the BSA control samples.

tive regulator of cell proliferation that promotes neuronal differentiation (16, 24, 28). The contribution of the altered expression of other candidate genes, such as *Igf2* (*I*nsulin-like *g*rowth *f*actor *II*) and *Phlda2* (*P*leckstrin *h*omology-*l*ike *d*omain, family *A*, member *2*), both of which have been implicated in growth control (12, 30), to the *Nap1l2* deletion phenotype remains to be ascertained. Interestingly, Cdkn1c acts as a cyclin kinase inhibitor in mitotic progenitor cells and is known to play a distinct role in neuronal differentiation (16, 24, 28). Our study shows that *Cdkn1c* is increasingly expressed during neuronal differentiation and that its upregulation is associated with increased histone H3K9/14 acetylation at its transcription start site. We have also shown that the Nap1l2 protein binds to the transcription start site of *Cdkn1c* and that in neurons from which *Nap1l2* was deleted, *Cdkn1c* becomes both downregulated and depleted in histone H3 acetylation. Our data suggest that Nap1l2 is involved in regulating *Cdkn1c* expression in neurons via regulation of histone acetylation. The functional importance of histone acetylation for *Cdkn1c*/*CDKN1C* expression, which is known to be regulated by various epigenetic marks (18, 31, 40), has also been suggested by the finding that the gene is silenced by histone deacetylation (18) and the increased expression of the gene in the presence of the deacetylase inhibitor TSA (36).

The role of the Nap1l2 protein at the *Cdkn1c* locus is likely a reflection of a more extensive role for Nap1l2 within the neuronal nucleus. The rather subtle transcriptional downregulation of *Cdkn1c* may indicate a role of Nap1l2 in the epigenetic modulation of basal transcription levels rather than in the specific activation of a subset of neurally expressed genes. Such a role would correlate with our finding that Nap1l2 interacts directly with the core histones H3 and H4 and increases both global and site-specific histone acetylation. Since the Nap1l2 protein itself has no intrinsic HAT activity (data not shown), one possibility is that it acts through activation of histone acetyltransferases such as p300 (7, 10), a protein which has the capacity to acetylate histone H3 and H4 both in vitro and in vivo (32). The previous finding of binding sites for the tumor suppressor p300 on the human *CDKN1C* promoter (36) is of obvious interest in this regard, as is the observation that mice nullizygous for p300, similar to *Nap1l2* knockout chimeras, die between days E9 and E11.5 of gestation and exhibit strong defects in neurulation and cell proliferation (41). It should be noted that the role for the neuron-specific Nap1l2 protein in histone acetylation that this leads us to propose is the somehow opposite of that described for the ubiquitously expressed NAP and SET proteins, which have been shown to inhibit HAT activity (2, 33). While Nap1l2 also has a particularly strong affinity for the acetylated forms of histones H3 and H4, possibly indicating a role in maintaining the acetylation status of histones, we have been unable to demonstrate a direct inhibitory effect of Nap1l2 on histone deacetylation in vitro (data not shown). Of relevance may be the fact that while Nap1l2 has two homology domains in common with other members of the NAP family (amino acids 96 to 159 and 235 to 377), it also contains a specific Glu-rich acidic domain (amino acids 160 to 234) that may well contribute to its unique functioning. A role of Nap1l2 in the establishment of other histone modifications remains to be shown. We interpret our preliminary evidence for a reduction in repressive histone H3 marks such as trimethyl H3K27 at the *Cdkn1c* locus in the presence of Nap1l2 (data not shown) as a likely secondary consequence of higher H3 acetylation levels.

The acetylation status of histones is thought to act as a general regulator of chromatin structure that mediates the removal of epigenetically controlled repression and enhances transcriptional activity. This is reflected by the finding that acetylated K9/14 of histone H3 is found to be highly localized to the 5′ regions of transcriptionally active human genes (20). Gene expression states depend on the binding of sequence-specific transcription factors and the recruitment of chromatin-remodeling complexes and can be modified during DNA replication and transcription (8). While studies provide evidence for general alterations in histone modification, such as the increased histone H3 and H4 acetylation occurring during neuronal differentiation (13), postmitotic neurons can no longer rely on a replication-dependent machinery to renew or modify their chromatin-bound histone pool. Chromatin modification-dependent gene expression patterns can, however, be established and maintained in such cells by certain histone variants, such as the hyperacetylated variant histone H3.3 (6), that can be incorporated into nucleosomes in a DNA replication-independent manner (1). During mitosis, histone modification and variant incorporation combine to set stable epigenetic marks for the memory of active transcriptional states (8).

Our findings suggest that Nap1l2 is involved in the dynamics of histone modification at its target loci during differentiation.

One possible mechanism could be that Nap1l2 facilitates the accessibility of HATs, such as p300, to histones, although the possibility that Nap1l2 might participate directly in the selective incorporation or exchange of hyperacetylated histones remains to be excluded (23). Irrespective of the precise mechanism, the resulting modulation in gene expression regulates the kinetics of neuronal differentiation, which is central to the process of neurulation. Our findings add another dimension of complexity to the potential role of the Nap1l2 molecule and reinforce the likelihood that other members of the mammalian neuronal NAP1-like proteins may be involved in a possibly complementary manner in regulating cellular activity via histone modifications. It remains to be shown whether such findings for Nap1l2 can be extended to the ubiquitous NAPs that are present not only in neurons but also in all other cell types.

ACKNOWLEDGMENTS

We are grateful to Marie Christine Wagner for helping with the FACS analysis and to Robert Olaso for advice on the microarray analysis. We thank Delphine Bohl for help with immunofluorescence, Claire Rougeulle and Pablo Navarro for the introduction to ChIP analysis, and Geneviève Almouzni, Angelita Rebollo, Matthieu Gérard, and Nicolas Zarjevski for critical reading of the manuscript.

This work was supported by grants from the ARC, AFM, and the EU Epigenome program (CE LSHG CT 2004 503433) and by recurrent funding from the CNRS, INSERM, and the Pasteur Institute (GPH7SP2). M.A. is recipient of a fellowship from the Cancéropôle, Ile de France.

REFERENCES

1. **Ahmad, K., and S. Henikoff.** 2002. The histone variant H3.3 marks active chromatin by replication-independent nucleosome assembly. Mol. Cell **9:**1191–1200.
2. **Asahara, H., S. Tartare-Deckert, T. Nakagawa, T. Ikehara, F. Hirose, T. Hunter, T. Ito, and M. Montminy.** 2002. Dual roles of p300 in chromatin assembly and transcriptional activation in cooperation with nucleosome assembly protein 1 in vitro. Mol. Cell. Biol. **22:**2974–2983.
3. **Aubert, J., M. P. Stavridis, S. Tweedie, M. O'Reilly, K. Vierlinger, M. Li, P. Ghazal, T. Pratt, J. O. Mason, D. Roy, and A. Smith.** 2003. Screening for mammalian neural genes via fluorescence-activated cell sorter purification of neural precursors from Sox1-gfp knock-in mice. Proc. Natl. Acad. Sci. USA **100**(Suppl. 1)**:**11836–11841.
4. **Balasubramaniyan, V., E. Boddeke, R. Bakels, B. Kust, S. Kooistra, A. Veneman, and S. Copray.** 2006. Effects of histone deacetylation inhibition on neuronal differentiation of embryonic mouse neural stem cells. Neuroscience **143:**939–951.
5. **Bieberich, E., S. MacKinnon, J. Silva, S. Noggle, and B. G. Condie.** 2003. Regulation of cell death in mitotic neural progenitor cells by asymmetric distribution of prostate apoptosis response 4 (PAR-4) and simultaneous elevation of endogenous ceramide. J. Cell Biol. **162:**469–479.
6. **Bosch, A., and P. Suau.** 1995. Changes in core histone variant composition in differentiating neurons: the roles of differential turnover and synthesis rates. Eur. J. Cell Biol. **68:**220–225.
7. **Chan, H. M., and N. B. La Thangue.** 2001. p300/CBP proteins: HATs for transcriptional bridges and scaffolds. J. Cell Sci. **114:**2363–2373.
8. **Chow, C. M., A. Georgiou, H. Szutorisz, A. Maia e Silva, A. Pombo, I. Barahona, E. Dargelos, C. Canzonetta, and N. Dillon.** 2005. Variant histone H3.3 marks promoters of transcriptionally active genes during mammalian cell division. EMBO Rep. **6:**354–360.
9. **Chureau, C., M. Prissette, A. Bourdet, V. Barbe, L. Cattolico, L. Jones, A. Eggen, P. Avner, and L. Duret.** 2002. Comparative sequence analysis of the X-inactivation center region in mouse, human, and bovine. Genome Res. **12:**894–908.
10. **Giordano, A., and M. L. Avantaggiati.** 1999. p300 and CBP: partners for life and death. J. Cell. Physiol. **181:**218–230.
11. **Graham, V., J. Khudyakov, P. Ellis, and L. Pevny.** 2003. SOX2 functions to maintain neural progenitor identity. Neuron **39:**749–765.
12. **Hartmann, W., A. Koch, H. Brune, A. Waha, U. Schuller, I. Dani, D. Denkhaus, W. Langmann, U. Bode, O. D. Wiestler, K. Schilling, and T. Pietsch.** 2005. Insulin-like growth factor II is involved in the proliferation control of medulloblastoma and its cerebellar precursor cells. Am. J. Pathol. **166:**1153–1162.
13. **Hsieh, J., K. Nakashima, T. Kuwabara, E. Mejia, and F. H. Gage.** 2004. Histone deacetylase inhibition-mediated neuronal differentiation of multipotent adult neural progenitor cells. Proc. Natl. Acad. Sci. USA **101:**16659–16664.
14. **Hu, R. J., M. P. Lee, L. A. Johnson, and A. P. Feinberg.** 1996. A novel human homologue of yeast nucleosome assembly protein, 65 kb centromeric to the p57KIP2 gene, is biallelically expressed in fetal and adult tissues. Hum. Mol. Genet. **5:**1743–1748.
15. **Ito, T., T. Ikehara, T. Nakagawa, W. L. Kraus, M. Muramatsu, M. Gos, and A. Szpecht-Potocka.** 2000. p300-mediated acetylation facilitates the transfer of histone H2A-H2B dimers from nucleosomes to a histone chaperone. Genes Dev. **14:**1899–1907.
16. **Joseph, B., A. Wallen-Mackenzie, G. Benoit, T. Murata, E. Joodmardi, S. Okret, and T. Perlmann.** 2003. p57(Kip2) cooperates with Nurr1 in developing dopamine cells. Proc. Natl. Acad. Sci. USA **100:**15619–15624.
17. **Kellogg, D. R., A. Kikuchi, T. Fujii-Nakata, C. W. Turck, and A. W. Murray.** 1995. Members of the NAP/SET family of proteins interact specifically with B-type cyclins. J. Cell Biol. **130:**661–673.
18. **Kikuchi, T., M. Toyota, F. Itoh, H. Suzuki, T. Obata, H. Yamamoto, H. Kakiuchi, M. Kusano, J. P. Issa, T. Tokino, and K. Imai.** 2002. Inactivation of p57KIP2 by regional promoter hypermethylation and histone deacetylation in human tumors. Oncogene **21:**2741–2749.
19. **Laskey, R. A., B. M. Honda, A. D. Mills, and J. T. Finch.** 1978. Nucleosomes are assembled by an acidic protein which binds histones and transfers them to DNA. Nature **275:**416–420.
20. **Liang, G., J. C. Lin, V. Wei, C. Yoo, J. C. Cheng, C. T. Nguyen, D. J. Weisenberger, G. Egger, D. Takai, F. A. Gonzales, and P. A. Jones.** 2004. Distinct localization of histone H3 acetylation and H3–K4 methylation to the transcription start sites in the human genome. Proc. Natl. Acad. Sci. USA **101:**7357–7362.
21. **Méndez, J., and B. Stillman.** 2000. Chromatin association of human origin recognition complex, Cdc6, and minichromosome maintenance proteins during the cell cycle: assembly of prereplication complexes in late mitosis. Mol. Cell. Biol. **20:**8602–8612.
22. **Navarro, P., S. Pichard, C. Ciaudo, P. Avner, and C. Rougeulle.** 2005. Tsix transcription across the Xist gene alters chromatin conformation without affecting Xist transcription: implications for X-chromosome inactivation. Genes Dev. **19:**1474–1484.
23. **Okuwaki, M., K. Kato, H. Shimahara, S. Tate, and K. Nagata.** 2005. Assembly and disassembly of nucleosome core particles containing histone variants by human nucleosome assembly protein I. Mol. Cell. Biol. **25:**10639–10651.
24. **Park, H. C., J. Boyce, J. Shin, and B. Appel.** 2005. Oligodendrocyte specification in zebrafish requires notch-regulated cyclin-dependent kinase inhibitor function. J. Neurosci. **25:**6836–6844.
25. **Park, Y. J., and K. Luger.** 2006. The structure of nucleosome assembly protein 1. Proc. Natl. Acad. Sci. USA **103:**1248–1253.
26. **Rodriguez, P., J. Pelletier, G. B. Price, and M. Zannis-Hadjopoulos.** 2000. NAP-2: histone chaperone function and phosphorylation state through the cell cycle. J. Mol. Biol. **298:**225–238.
27. **Rogner, U. C., D. D. Spyropoulos, N. Le Novere, J. P. Changeux, and P. Avner.** 2000. Control of neurulation by the nucleosome assembly protein-1-like 2. Nat. Genet. **25:**431–435.
28. **Rothschild, G., X. Zhao, A. Iavarone, and A. Lasorella.** 2006. E proteins and Id2 converge on p57Kip2 to regulate cell cycle in neural cells. Mol. Cell. Biol. **26:**4351–4361.
29. **Rougeulle, C., and P. Avner.** 1996. Cloning and characterization of a murine brain specific gene Bpx and its human homologue lying within the Xic candidate region. Hum. Mol. Genet. **5:**41–49.
30. **Salas, M., R. John, A. Saxena, S. Barton, D. Frank, G. Fitzpatrick, M. J. Higgins, and B. Tycko.** 2004. Placental growth retardation due to loss of imprinting of Phlda2. Mech. Dev. **121:**1199–1210.
31. **Sato, N., H. Matsubayashi, T. Abe, N. Fukushima, and M. Goggins.** 2005. Epigenetic down-regulation of CDKN1C/p57KIP2 in pancreatic ductal neoplasms identified by gene expression profiling. Clin. Cancer Res. **11:**4681–4688.
32. **Schiltz, R. L., C. A. Mizzen, A. Vassilev, R. G. Cook, C. D. Allis, and Y. Nakatani.** 1999. Overlapping but distinct patterns of histone acetylation by the human coactivators p300 and PCAF within nucleosomal substrates. J. Biol. Chem. **274:**1189–1192.
33. **Seo, S. B., P. McNamara, S. Heo, A. Turner, W. S. Lane, and D. Chakravarti.** 2001. Regulation of histone acetylation and transcription by INHAT, a human cellular complex containing the set oncoprotein. Cell **104:**119–130.
34. **Shikama, N., H. M. Chan, M. Krstic-Demonacos, L. Smith, C. W. Lee, W. Cairns, and N. B. La Thangue.** 2000. Functional interaction between nucleosome assembly proteins and p300/CREB-binding protein family coactivators. Mol. Cell. Biol. **20:**8933–8943.
35. **Simon, H. U., G. B. Mills, M. Kozlowski, D. Hogg, D. Branch, Y. Ishimi, and K. A. Siminovitch.** 1994. Molecular characterization of hNRP, a cDNA encoding a human nucleosome-assembly-protein-I-related gene product involved in the induction of cell proliferation. Biochem. J. **297:**389–397.
36. **Smith, J. L., W. J. Freebern, I. Collins, A. De Siervi, I. Montano, C. M. Haggerty, M. C. McNutt, W. G. Butscher, I. Dzekunova, D. W. Petersen, E.**

Kawasaki, J. L. Merchant, and K. Gardner. 2004. Kinetic profiles of p300 occupancy in vivo predict common features of promoter structure and coactivator recruitment. Proc. Natl. Acad. Sci. USA **101:**11554–11559.
37. **Smith, R. J., W. Dean, G. Konfortova, and G. Kelsey.** 2003. Identification of novel imprinted genes in a genome-wide screen for maternal methylation. Genome Res. **13:**558–569.
38. **Taniguchi, M., M. Sanbo, S. Watanabe, I. Naruse, M. Mishina, and T. Yagi.** 1998. Efficient production of Cre-mediated site-directed recombinants through the utilization of the puromycin resistance gene, pac: a transient gene-integration marker for ES cells. Nucleic Acids Res. **26:**679–680.
39. **Watanabe, T. K., T. Fujiwara, Y. Nakamura, Y. Hirai, H. Maekawa, and E. Takahashi.** 1996. Cloning, expression pattern and mapping to Xq of NAP1L3, a gene encoding a peptide homologous to human and yeast nucleosome assembly proteins. Cytogenet. Cell Genet. **74:**281–285.
40. **Yang, H., K. Hoshino, B. Sanchez-Gonzalez, H. Kantarjian, and G. Garcia-Manero.** 2005. Antileukemia activity of the combination of 5-aza-2′-deoxycytidine with valproic acid. Leuk. Res. **29:**739–748.
41. **Yao, T. P., S. P. Oh, M. Fuchs, N. D. Zhou, L. E. Ch'ng, D. Newsome, R. T. Bronson, E. Li, D. M. Livingston, and R. Eckner.** 1998. Gene dosage-dependent embryonic development and proliferation defects in mice lacking the transcriptional integrator p300. Cell **93:**361–372.
42. **Yeo, W., and J. Gautier.** 2004. Early neural cell death: dying to become neurons. Dev. Biol. **274:**233–244.
43. **Ying, Q. L., M. Stavridis, D. Griffiths, M. Li, and A. Smith.** 2003. Conversion of embryonic stem cells into neuroectodermal precursors in adherent monoculture. Nat. Biotechnol. **21:**183–186.
44. **Zhang, P., N. J. Liegeois, C. Wong, M. Finegold, H. Hou, J. C. Thompson, A. Silverman, J. W. Harper, R. A. DePinho, and S. J. Elledge.** 1997. Altered cell differentiation and proliferation in mice lacking p57KIP2 indicates a role in Beckwith-Wiedemann syndrome. Nature **387:**151–158.